Supplemental Figure Legends

Figure S1. Detailed structural comparison of the post-SET from the autoinhibited *ct*PRC2 (*top*) with the stimulated state structures (*bottom*, PDB ID: 5KKL). Residues are labeled in gold (*post-SET*) or magenta (*H3 peptide*).

Figure S2. Crystal packing of autoinhibited *ct*PRC2, with proteins color-coded. The post-SET sub-domain (*dark blue cartoon marked by the black arrow*) of *ct*Ezh2 is not involved in crystal packing and is located far away from *ct*PRC2 symmetry mates (*gray ribbons*).

Figure S3. Structural alignment of Ezh2 SET domains from *ct*PRC2 stimulated (*gray*, PDB ID: 5KKL) and autoinhibited (*blue*) states. Dashed, black lines indicate un-modeled regions. Several residues within amino acids 848-855 of the SET-I are shown as sticks to indicate conformational changes between the two states.

Figure S4. The post-SET region (*gold*) is stabilized by an extensive network of direct and water-mediated hydrogen bonds with the SET-I region (*cyan*) in the autoinhibited state. Important residues are shown as sticks, waters are depicted as red spheres, and black, dotted lines indicate hydrogen bonds.

Figure S5. Detailed comparison of the SAM binding site between the ctPRC2 SAM-bound and stimulated (PDB ID: 5KKL) structures. Hydrogen bonds are indicated by black, dashed lines. The side-chain of C807 is omitted for clarity. The post-SET region of the SAM-bound structure is not shown because it does not participated in SAM binding.

Figure S6. SDS-PAGE analysis of proteins used in biochemical assays. A) Proteins from Fig. 2B. B) Proteins from SAL mutational analysis, Fig. 2D. C) Proteins from autoinhibition mutational analysis, Fig. 3A. D) Proteins used for kinetic analysis, Figs. 3D and 3E, and for crystallization.

Figure S7. B-factor analysis of autoinhibited wildtype *ct*PRC2 (*top*) and E840A_K852D mutant (*bottom*). B-factors are heat-colored from dark-blue (*relative lowest*) to red (*relative highest*). The view is the same as **Fig. 4**.

Figure S8. Sequence alignment of human (*h*) and *ct*Ezh2. The SET-I (*cyan*)

and post-SET (*gold*) subdomains are indicated by dashed boxes. Purple stars indicate aromatic cage residues of the active site. Red hexagons indicate residues important for autoinhibition in *ct*PRC2.

Figure S9. Structural alignment of the autoinhibited SET domains of *ct*Ezh2 and *h*Ezh2. **(A)** Comparison with an isolated *h*Ezh2(SET) (PDB ID: 4MI5). For simplicity, only the post-SET (*gold in ctEzh2* and *blue in human*) and SET-I (*green in human*) are color-coded. Black, dashed lines indicate hydrogen bonds. Placement of the histone H3K27M peptide (*magenta*) is based on alignment with the substrate bound human structure (PDB ID: 5HYN). Hydrogen bonds are indicated by black, dashed lines. **(B)** Comparison with hEzh2(SET) in an active autoinhibited *h*PRC2 (*light gray*, PDB ID: 5IJ7). Formatting and color-coding is the same as for **(A)**.

Fig. S1

Bratkowski et al.

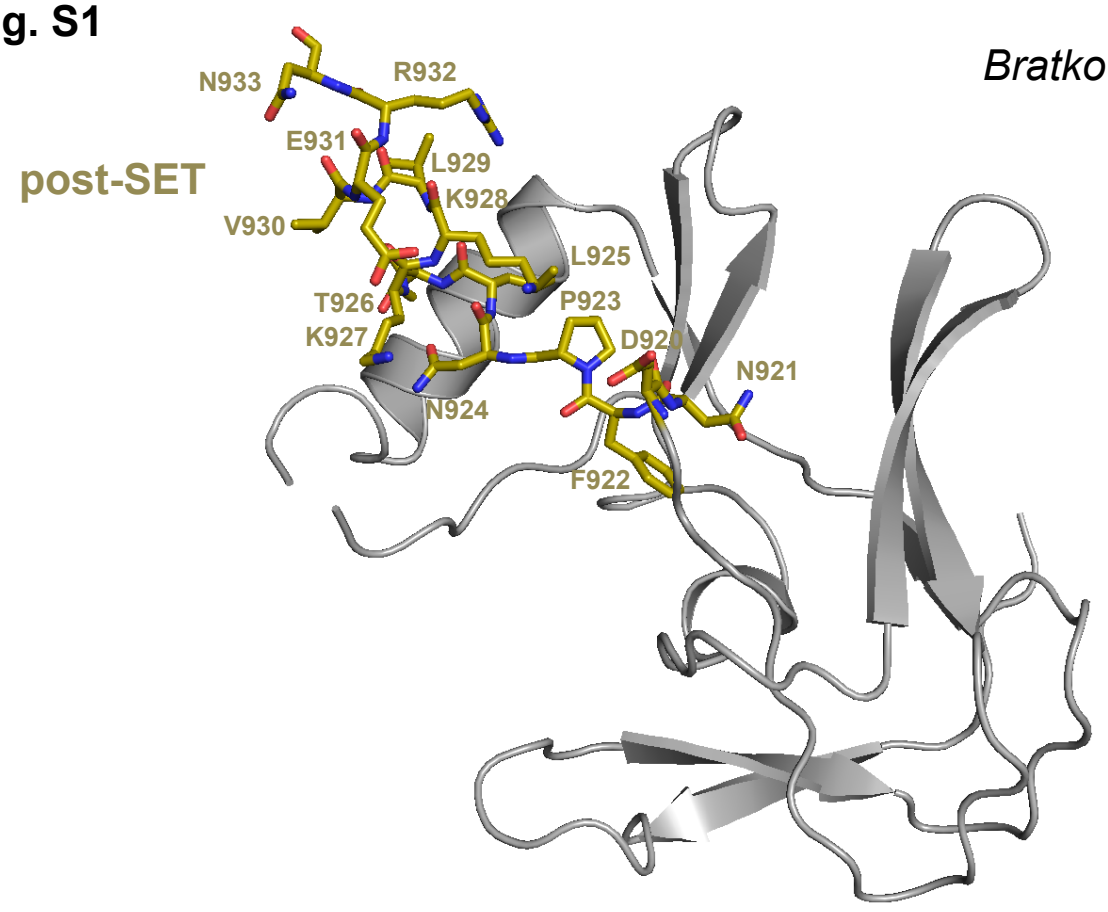

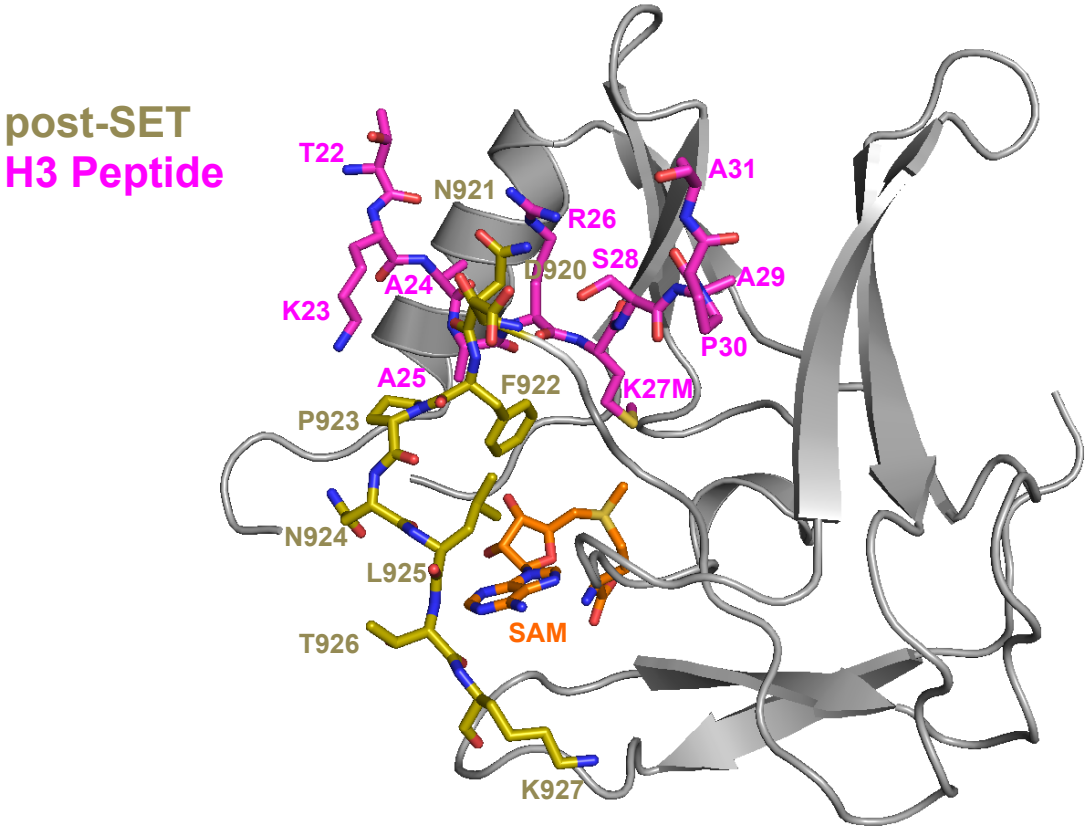

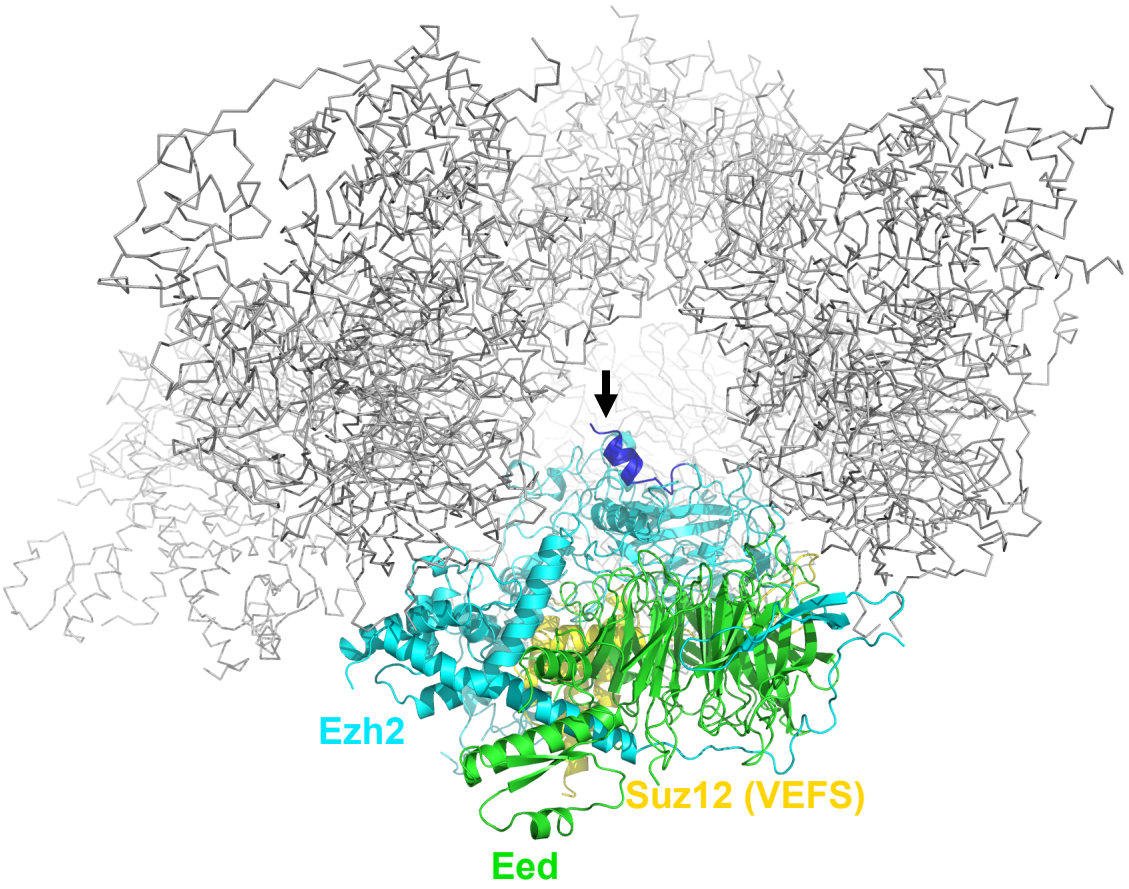
Ezh2
Suz12 (VEFS)
Eed

Fig. S3 *Bratkowski et al.*

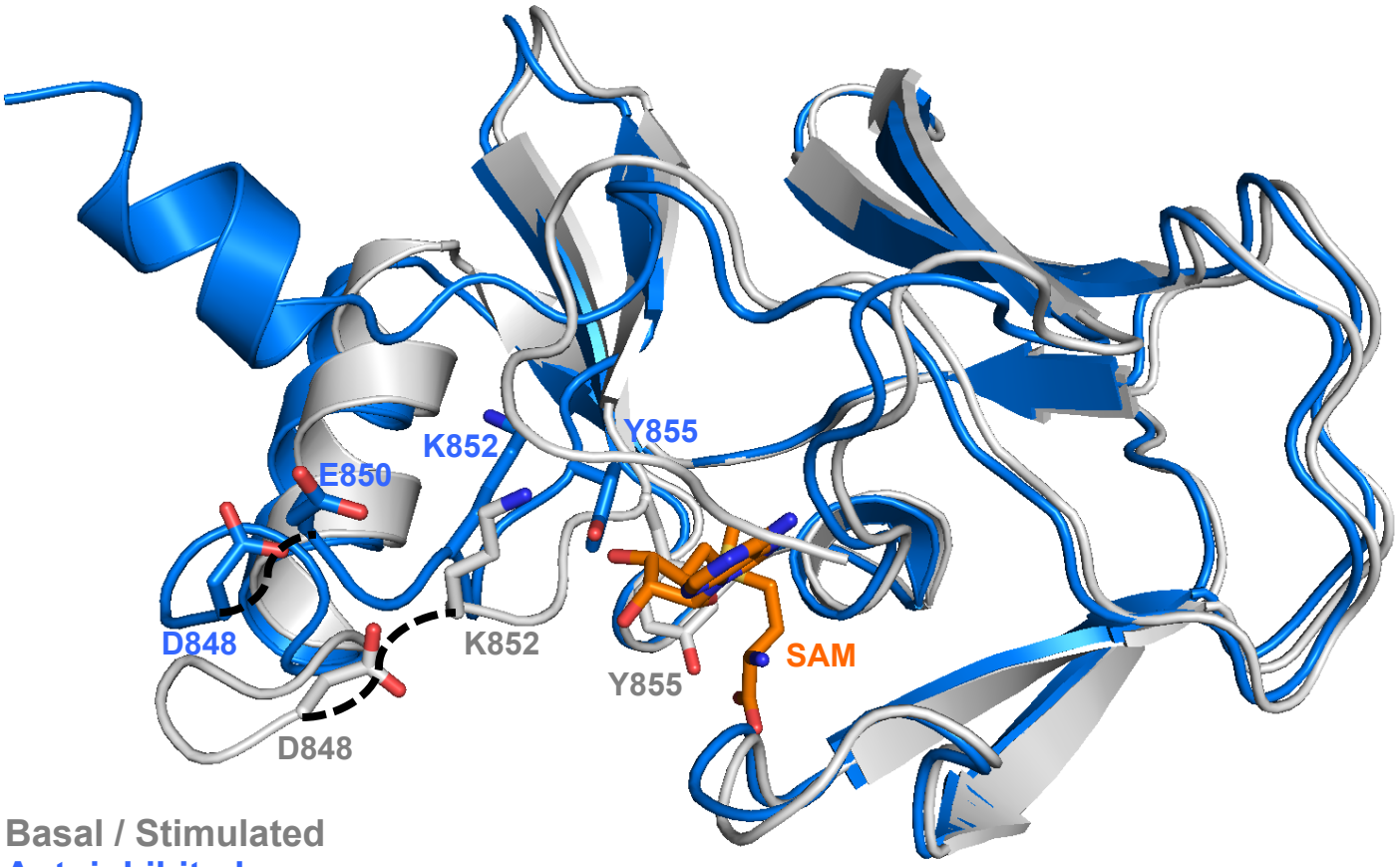

Fig. S4 *Bratkowski et al.*

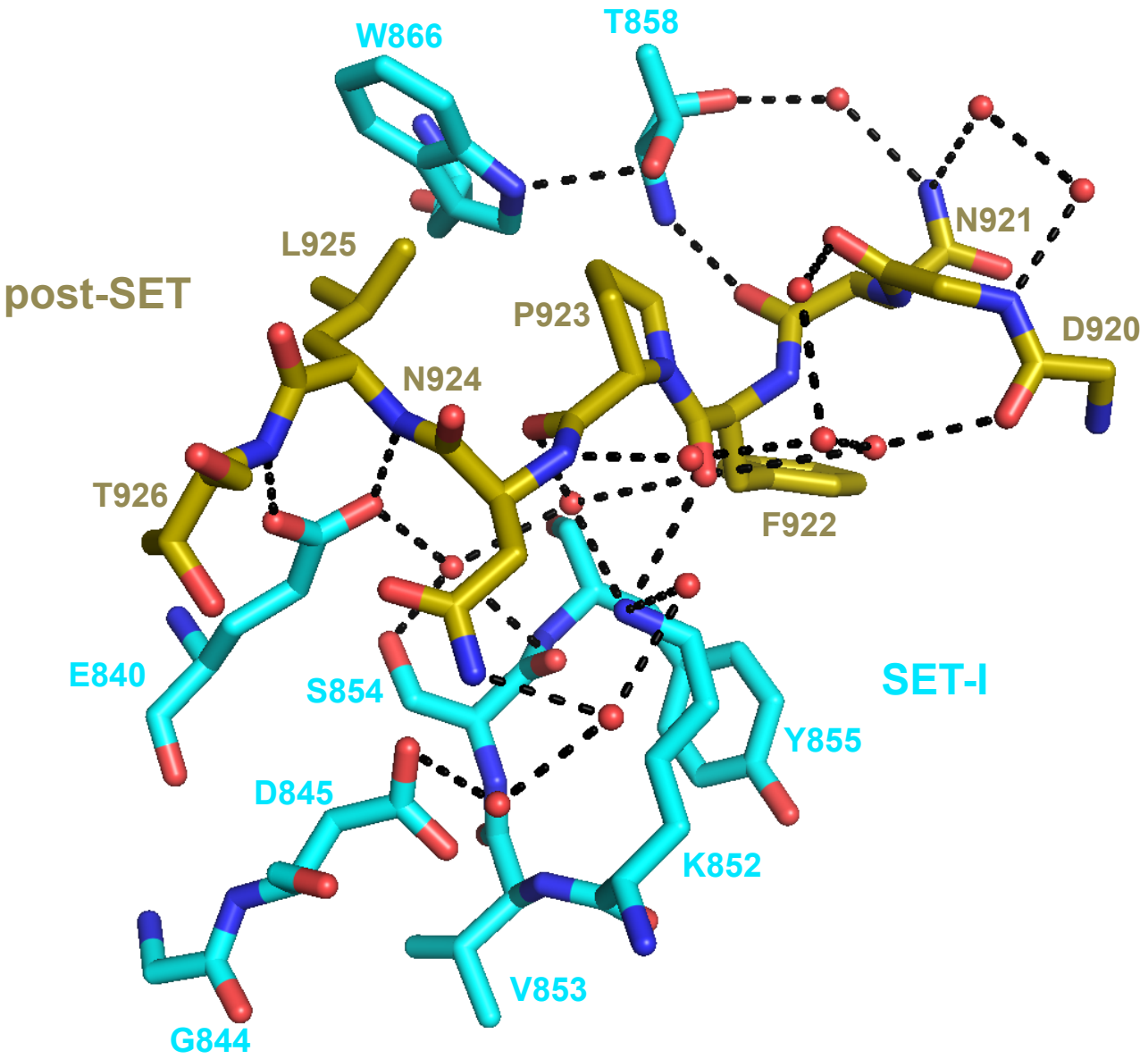

Fig. S5

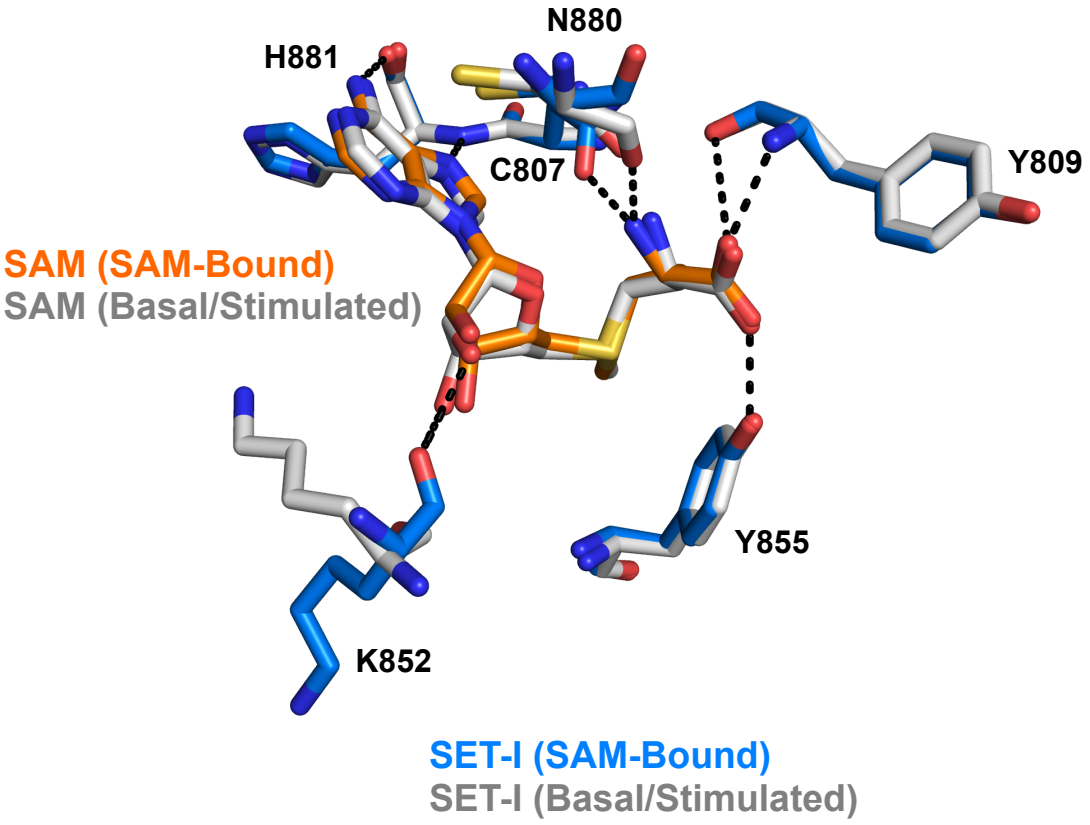
N880
H881
C807
Y809
SAM (SAM-Bound)
SAM (Basal/Stimulated)
Y855
K852
SET-I (SAM-Bound)
SET-I (Basal/Stimulated)

Fig. S6

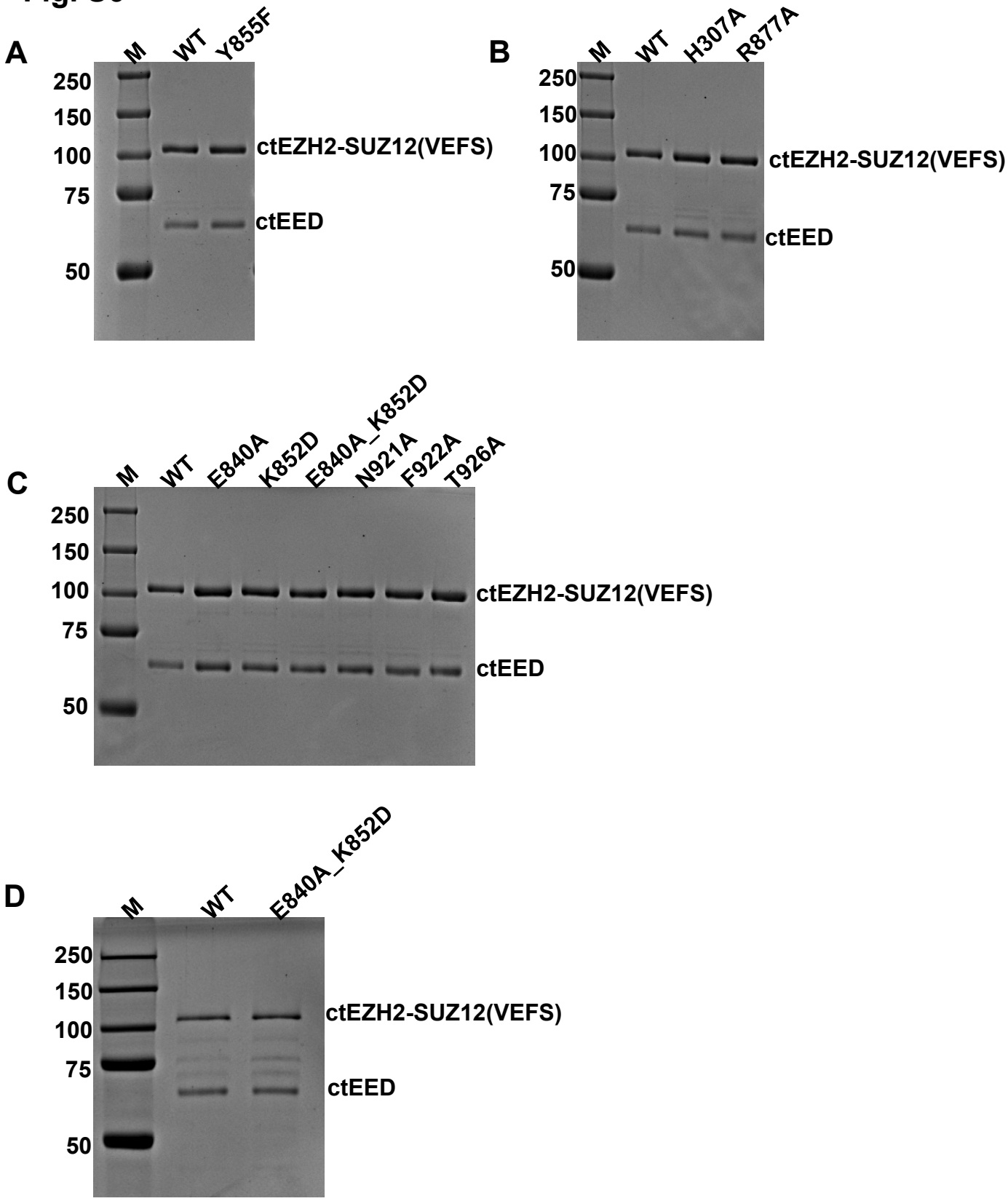
A
M
WT
Y855F
250
150
100
75
50
ctEZH2-SUZ12(VEFS)
ctEED
B
M
WT
H307A
R877A
250
150
100
75
50
ctEZH2-SUZ12(VEFS)
ctEED
C
M
WT
E840A
K852D
E840A_K852D
N921A
F922A
T926A
250
150
100
75
50
ctEZH2-SUZ12(VEFS)
ctEED
D
M
WT
E840A_K852D
250
150
100
75
50
ctEZH2-SUZ12(VEFS)
ctEED

Fig. S7

Wildtype

Bratkowski et al.

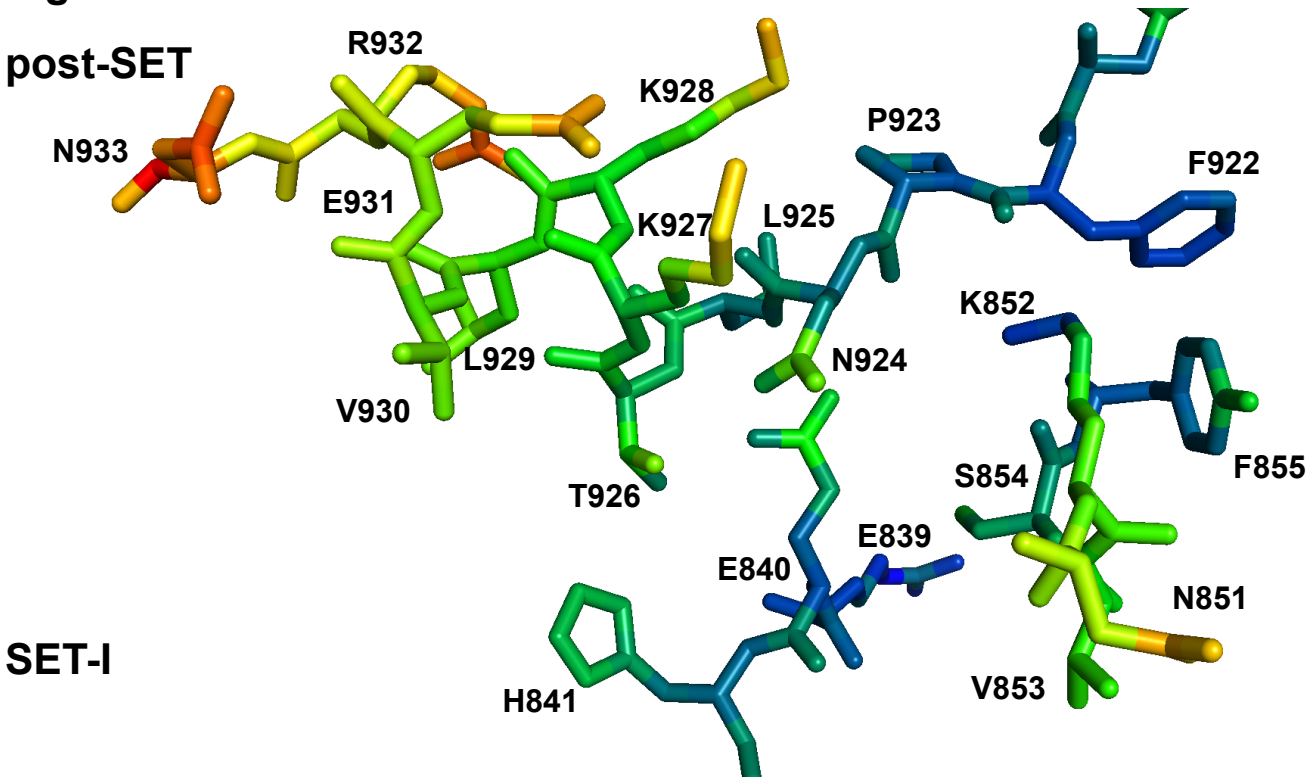

E840A/K852D

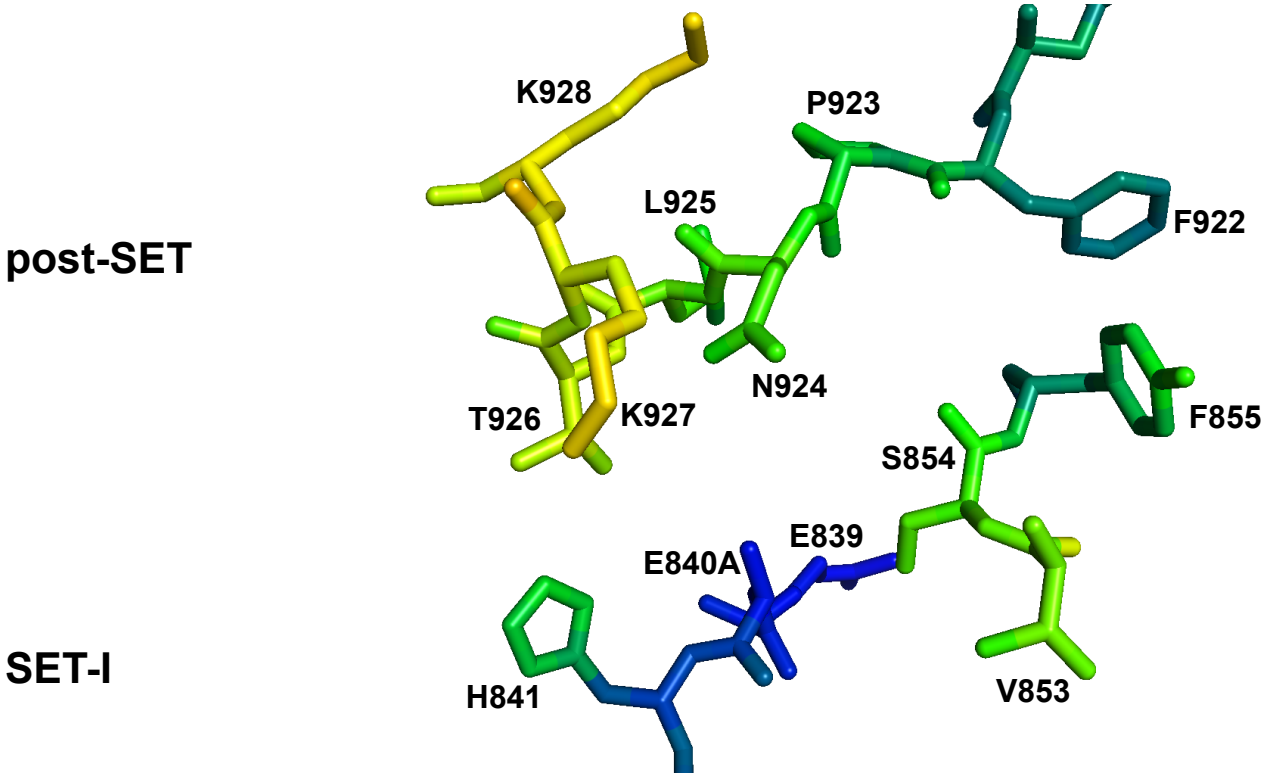

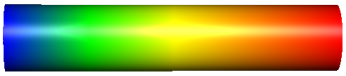

B-factor (Å^2) 23 133

Fig. S8

Bratkowski et al.

A

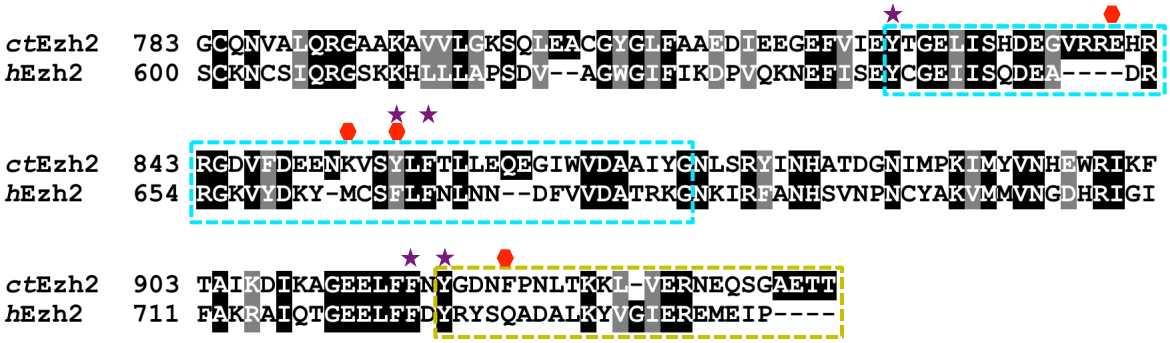

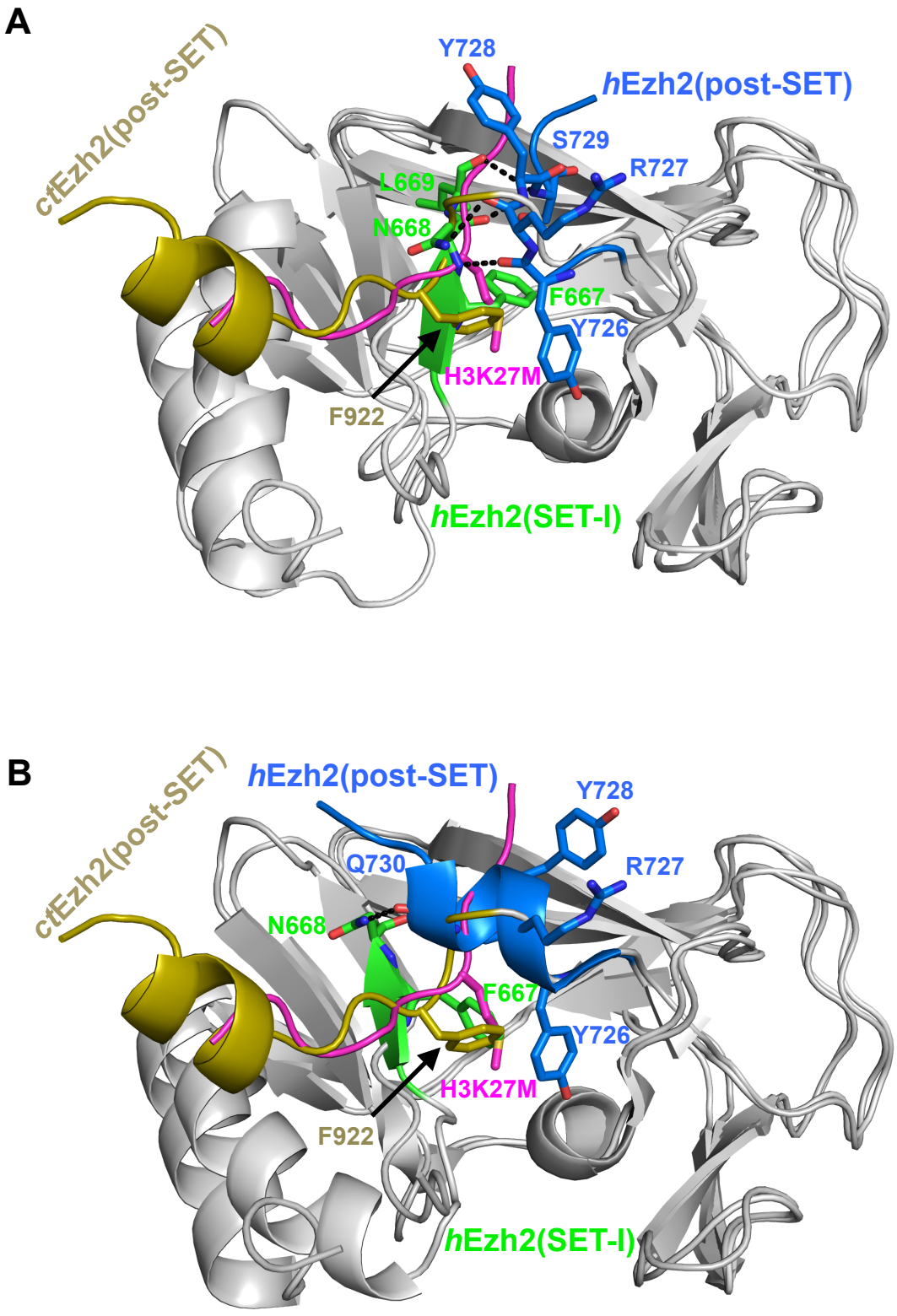
A
ctEzh2(post-SET)
Y728
hEzh2(post-SET)
S729
R727
L669
N668
F667
Y726
H3K27M
F922
hEzh2(SET-I)
B
ctEzh2(post-SET)
hEzh2(post-SET)
Y728
Q730
R727
N668
F667
Y726
H3K27M
F922
hEzh2(SET-I)

Table 1 Data collection and refinement statistics (molecular replacement)

Crystal	ctPRC2 WT Apo	ctPRC2 SAM	ctPRC2 E840/K852 Apo
Data collection[a]			
Space group	$C222_1$	$C222_1$	$C222_1$
Cell dimensions			
a, *b*, *c* (Å)	117.78, 137.90, 223.85	117.45, 138.01, 223.063	117.59, 138.00, 224.37
α, β, γ (°)	90, 90, 90	90, 90, 90	90, 90, 90
Resolution (Å)	50 – 2.19 (2.25 – 2.19)	50 – 2.57 (2.64 – 2.57)	50 – 2.12 (2.16 – 2.11)[b]
R_{merge}	0.126 (1.54)	0.162 (1.40)	0.237 (3.86)
R_{pim}	0.052 (0.66)	0.057 (0.49)	0.067 (1.09)
$I / \sigma I$	14.91 (1.33)	12.79 (1.63)	23.13 (1.59)
$CC_{1/2}$	0.81 (0.42)	0.89 (0.55)	0.88 (0.465)
Completeness (%)	99.9 (99.8)	99.6 (99.6)	100 (100)
Redundancy	6.7 (6.2)	8.9 (9.0)	13.2 (13.4)
Refinement			
Resolution (Å)	43.45 – 2.19 (2.25 – 2.18)	47.32 – 2.57 (2.64 – 2.57)	44.75 – 2.11 (2.16 – 2.11)
No. reflections	89879	55206	98691
R_{work} / R_{free}	0.173/0.224	0.174/0.232	0.168/0.214
No. atoms	10825	10500	10991
Protein	10028	10221	10083
Ligand/ion	8	35	8
Water	789	244	900
Ave. *B*-factors (Å^2)			
Protein	45.31	53.05	37.22
Ligand/ion	39.12	46.03	29.23
Water	46.08	45.65	39.57
R.m.s. deviations			
Bond lengths (Å)	0.009	0.009	0.008
Bond angles (°)	0.884	0.990	0.845
Ramachandran Plot			
Favored (%)	96.60	95.54	95.80
Allowed (%)	3.23	3.98	3.96
Outlier (%)	0.16	0.48	0.24

[a]Data were collected from a single crystal. [b]Values in parentheses are for highest-resolution shell.